The proarrhythmic features of pathological cardiac hypertrophy in neonatal rat ventricular cardiomyocyte cultures

Neshati, Z.; Schalij, M.J.; Vries, A.A.F. de

Citation
Neshati, Z., Schalij, M. J., & Vries, A. A. F. de. (2020). The proarrhythmic features of pathological cardiac hypertrophy in neonatal rat ventricular cardiomyocyte cultures. *Journal Of Applied Physiology, 128*(3), 545-553. doi:10.1152/japplphysiol.00420.2019

Version: Publisher's Version
License: Creative Commons CC BY 4.0 license
Downloaded from: https://hdl.handle.net/1887/3232727

Note: To cite this publication please use the final published version (if applicable).

J Appl Physiol 128: 545–553, 2020.
First published January 30, 2020; doi:10.1152/japplphysiol.00420.2019.

RESEARCH ARTICLE

The proarrhythmic features of pathological cardiac hypertrophy in neonatal rat ventricular cardiomyocyte cultures

Zeinab Neshati,[1,2] Martin J. Schalij,[2] and Antoine A. F. de Vries[2]

[1]*Zeinab Neshati, Department of Biology, Faculty of Science, Ferdowsi University of Mashhad, Mashhad, Iran; and*
[2]*Laboratory of Experimental Cardiology, Department of Cardiology, Heart Lung Center Leiden, Leiden University Medical Center, Leiden, The Netherlands*

Submitted 17 June 2019; accepted in final form 28 January 2020

Neshati Z, Schalij MJ, de Vries AAF. The proarrhythmic features of pathological cardiac hypertrophy in neonatal rat ventricular cardiomyocyte cultures. *J Appl Physiol* 128: 545–553, 2020. First published January 30, 2020; doi:10.1152/japplphysiol.00420.2019.—Different factors may trigger arrhythmias in diseased hearts, including fibrosis, cardiomyocyte hypertrophy, hypoxia, and inflammation. This makes it difficult to establish the relative contribution of each of them to the occurrence of arrhythmias. Accordingly, in this study, we used an in vitro model of pathological cardiac hypertrophy (PCH) to investigate its proarrhythmic features and the underlying mechanisms independent of fibrosis or other PCH-related processes. Neonatal rat ventricular cardiomyocyte (nr-vCMC) monolayers were treated with phorbol 12-myristate 13-acetate (PMA) to create an in vitro model of PCH. The electrophysiological properties of PMA-treated and control monolayers were analyzed by optical mapping at *day 9* of culture. PMA treatment led to a significant increase in cell size and total protein content. It also caused a reduction in sarcoplasmic/endoplasmic reticulum Ca^{2+} ATPase 2 level (32%) and an increase in natriuretic peptide A (42%) and α1-skeletal muscle actin (34%) levels, indicating that the hypertrophic response induced by PMA was, indeed, pathological in nature. PMA-treated monolayers showed increases in action potential duration (APD) and APD dispersion, and a decrease in conduction velocity (CV; APD_{30} of 306 ± 39 vs. 148 ± 18 ms, APD_{30} dispersion of 85 ± 19 vs. 22 ± 7 and CV of 10 ± 4 vs. 21 ± 2 cm/s in controls). Upon local 1-Hz stimulation, 53.6% of the PMA-treated cultures showed focal tachyarrhythmias based on triggered activity (n = 82), while the control group showed 4.3% tachyarrhythmias (n = 70). PMA-treated nr-vCMC cultures may, thus, represent a well-controllable in vitro model for testing new therapeutic interventions targeting specific aspects of hypertrophy-associated arrhythmias.

NEW & NOTEWORTHY Phorbol 12-myristate 13-acetate (PMA) treatment of neonatal rat ventricular cardiomyocytes (nr-vCMCs) led to induction of many significant features of pathological cardiac hypertrophy (PCH), including action potential duration prolongation and dispersion, which provided enough time and depolarizing force for formation of early afterdepolarization (EAD)-induced focal tachyarrhythmias. PMA-treated nr-vCMCs represent a well-controllable in vitro model, which mostly resembles to moderate left ventricular hypertrophy (LVH) rather than severe LVH, in which generation of a reentry is the putative mechanism of its arrhythmias.

cell culture; pathological cardiac hypertrophy; phorbol 12-myristate 13-acetate; triggered activity

INTRODUCTION

An increase in cardiac demand triggers the heart to respond in several ways, including by the enlargement of cardiomyocytes. Such cardiac hypertrophy is essentially a beneficial compensatory process, as it decreases wall stress, while increasing cardiac output (18). This adaptation by growth occurs under physiological conditions like exercise and pregnancy, but also in response to myocardial infarction and other cardiac pathologies. Whereas physiological cardiac hypertrophy is usually reversible and contributes to optimal heart function, hypertrophy due to cardiac disease [i.e., pathological cardiac hypertrophy (PCH)] is typically associated with several irreversible time-dependent detrimental changes, including maladaptive remodeling of cardiac structure, metabolism, electrophysiology, and ion homeostasis, which may ultimately culminate in heart failure (9, 29, 52). Electrophysiological remodeling, especially if sustained, imposes an increased risk of developing cardiac arrhythmias.

The relationship of PCH with ventricular tachyarrhythmias has been investigated in whole heart mapping studies (4, 17, 19, 28). However, the complexity of three-dimensional (3D) myocardial tissue and the presence in pathologically hypertrophied hearts of various other changes in cardiac structure and function, including fibrosis, inflammation, and metabolic remodeling (2, 28), complicates assessment of the specific contribution of PCH to the development of heart rhythm disturbances. This problem can be overcome by using two-dimensional (2D) cell culture models of defined composition to study PCH-related proarrhythmic changes. Induction of hypertrophy-related pathological changes in cardiomyocyte cultures can be accomplished by exposure of the cells to a variety of different peptide and nonpeptide hormones and growth factors, including ANG II, endothelin 1 (ET-1), and certain natural and synthetic catecholamines (40). Many of these molecules exert their prohypertrophic effects through the activation of phospholipase C, leading to the production of inositol 1,4,5-trisphosphate (IP_3) and diacylglycerol (DAG). Binding of IP_3 to specific receptors located in the membranes of the sarcoplasmic reticulum and in the nuclear envelope causes Ca^{2+} release into the cytosol and nucleus and activation of several prohypertrophic factors including calcineurin, nuclear factor of activated T cells (NFAT) and Ca^{2+}/calmodulin-dependent protein kinase II (CaMKII) (21). DAG, on the other hand, stimulates cardiac hypertrophy mainly by acting as stimulatory cofactor of protein kinase C (PKC) and protein kinase D (PKD)

Address for reprint requests and other correspondence: Z. Neshati, Dept. of Biology, Faculty of Science, Ferdowsi Univ. of Mashhad, Mashhad, Iran (e-mail: neshati@um.ac.ir).

8750-7587/20 Copyright © 2020 the American Physiological Society

Downloaded from journals.physiology.org/journal/jappl at Leids Univers Medisch Centrum (132.229.250.125) on January 11, 2023.

(45, 47). The prohypertrophic effects of DAG can be mimicked by phorbol 12-myristate 13-acetate (PMA). Indeed, treatment of neonatal rat ventricular cardiomyocytes (nr-vCMCs) with PMA has been shown to induce a gene expression program in these cells sharing many features with that of pathologically hypertrophied hearts (14, 35, 44). Prominent among the PMA-induced changes are those involving the expression level, cellular localization, and specific activity of ion channels and transporters (36, 42), connexins (13, 23), and Ca^{2+}-handling proteins (6, 34, 37) similar to what happens in pathologically hypertrophied hearts. Still, relatively little is known about the possible proarrhythmic consequences of these changes, which are commonly referred to as electrical remodeling. Therefore, the purpose of the present study was to investigate in PMA-treated nr-vCMC cultures the contribution of PCH to the development of cardiac arrhythmias independent of fibrosis, inflammation, and hypoxia.

MATERIALS AND METHODS

All animal experiments had the approval of the Animal Experiments Committee of the Leiden University Medical Center and complied with the Guide for the Care and Use of Laboratory Animals as stated by the U.S. National Institutes of Health.

Cardiomyocyte isolation. nr-vCMCs were isolated and cultured essentially, as described previously (33). In brief, two-day-old Wistar rats were anesthetized with 4–5% isoflurane. After confirmation of anesthesia, the chest was opened, the heart was excised, and the ventricles were separated from the remainder of the cardiac tissue. Next, the ventricular myocardium was cut into small pieces (~1 mm) and further dissociated by incubation at 37°C with a buffer solution containing 0.01 mM $CaCl_2$, 5 mM $MgCl_2$, 450 units/ml of collagenase 1 (Worthington, Lakewood, NJ) and 18.75 Kunitz units/ml DNase I (Sigma-Aldrich, St. Louis, MO). Cells and remaining tissue fragments were pelleted by centrifugation at 161 *g* and room temperature (RT) for 10 min and resuspended in growth medium [Ham's F10 medium supplemented with 10% fetal bovine serum (FBS) and 10% horse serum (HS; all from Life Technologies, Bleiswijk, the Netherlands)]. The cell suspension was then applied to Primaria culture dishes (Corning Life Sciences, Amsterdam, The Netherlands) and incubated for 75 min in a humidified incubator at 37°C and 5% CO_2 to allow preferential attachment of nonmyocytes. The unattached cells (mainly cardiomyocytes) were collected, passed through a cell strainer (70-μm mesh pore size; BD Biosciences, Breda, the Netherlands) to obtain a single-cell suspension and applied at a density of 6×10^5 cells/well of a 24-well cell culture plate (Corning Life Sciences) to fibronectin (Sigma-Aldrich)-coated, round glass coverslips (15-mm diameter). One day later (i.e., at culture *day 1*), the cells were treated in growth medium with mitomycin C (10 μg/ml; Sigma-Aldrich) for 2 h to inhibit proliferation of remaining nonmyocytes. The growth medium was subsequently replaced by a 1:1 mixture of Dulbecco's modified Eagle's medium (DMEM; Life Technologies) and Ham's F10 medium supplemented with 5% HS, 2% bovine serum albumin (BSA) and sodium ascorbate to a final concentration of 0.4 mM. This so-called maintenance medium was refreshed daily. To induce pathological hypertrophy, cultures were exposed to 1 μM PMA (BioVision, Milpitas, CA) for 24 h, at *days 3* and *8* of culture. Cell viability was assessed by 3-(4,5-dimethylthiazol-2-yl)-2,5-diphenyl tetrazolium bromide (MTT) assay at *day 9*.

In vitro cytotoxicity assay. The MTT assay was used to determine the cytotoxic effects of PMA. nr-vCMCs were seeded at a density of 2×10^5 cell/well in 96-well tissue culture plates, and three wells were used for each sample. The MTT dye (Sigma-Aldrich) was dissolved in phosphate-buffered saline (PBS; 5 mg/mL) and added to each well (20 μL/well), and the plates were incubated for 4 h, at 37°C. The reaction was then stopped by the addition of dimethyl sulfoxide (DMSO) (150 μL/well), and optic densities of the wells were measured spectrophotometrically at 570 nm using an enzyme-linked immunosorbent assay plate reader (Awareness, NY). Data were obtained from three independent nr-vCMCs isolation.

Optical mapping. Optical mapping was done at *day 9* of culture. Prior to optical mapping, the cells were incubated for 10 min in maintenance medium containing 8 μM of the voltage-sensitive dye di-4-ANEPPS (Life Technologies) and given fresh medium consisting of DMEM/HAM's F12 (Life Technologies) without phenol red and serum. Immediately afterward, cultures were optically mapped at 37°C using a MiCAM ULTIMA-L imaging system (SciMedia, Costa Mesa, CA). To allow for a fair comparison of action potential duration (APD) and conduction velocity (CV), all cultures were locally stimulated at 1 Hz using an epoxy-coated bipolar platinum electrode with square suprathreshold (i.e., 8 V) electrical stimuli of 10 ms. Parameters of interest were calculated using Brain Vision Analyzer 1208 software (Brainvision, Tokyo, Japan). Optical signals of nine pixels were averaged to minimize noise artifacts. To calculate CV, two 3 × 3 pixel grids located 2–8 mm apart on a line perpendicular to the activation wave front were used. APD was calculated at 30% (APD_{30}) and 80% (APD_{80}) of repolarization. CV and APD values were averages of values obtained from six different positions equally distributed across the cell cultures. APD_{30} and APD_{80} dispersion was expressed as the standard deviation (SD) of the mean of the APDs. For determining CV and APD and APD dispersion only nr-vCMC cultures with uniform activation patterns were used. Occurrence of proarrhythmic features was also evaluated after 1-Hz local stimulation. An early afterdepolarization (EAD) was defined as a reversal of repolarization during phase 2 or 3 of the AP of more than 10% of the maximum optical signal amplitude. A focal tachyarrhythmia was defined as an activation pattern in which an EAD was followed by two or more uninterrupted oscillations in membrane potential without giving rise to a reentrant circuit.

Immunocytology. For immunostaining, 8×10^4 cells were seeded on fibronectin-coated, round glass coverslips (15-mm diameter) in wells of 12-well cell culture plates (Corning Life Sciences). At *day 9* of culture, cells were fixed by incubation for 30 min in phosphate-buffered 4% formaldehyde (Klinipath, Duiven, the Netherlands) and permeabilized by a 20-min treatment with 0.1% Triton X-100 in PBS both at RT. Next, cells were incubated overnight at 4°C with mouse anti-sarcomeric α-actinin (clone: EA-53; Sigma-Aldrich), mouse anti-sarcoplasmic/endoplasmic reticulum Ca^{2+} ATPase 2 (Serca2; clone: 2A7-A1; Thermo Fisher Scientific, Waltham, MA, USA), rabbit anti-natriuretic peptide precursor type A (Nppa; Merck Millipore, order number: AB5490) and rabbit anti-α1-skeletal muscle actin (Acta1; Abcam, Cambridge, United Kingdom, order number: ab52218) primary antibodies diluted 1:200 in PBS + 0.1% donkey serum (Santa Cruz Biotechnology, Dallas, TX, USA) followed by a 2-h incubation at RT with appropriate Alexa Fluor 488- or 568-conjugated donkey IgG (H^+L) secondary antibodies (Life Technologies) diluted 1:400 in PBS + 0.1% donkey serum. Nuclei were counterstained with 10 μg/ml Hoechst 33342 (Life Technologies) in PBS. Cells were washed three times with PBS after fixation, permeabilization, and incubation with primary antibody, secondary antibody, and DNA-binding fluorochrome. To minimize photobleaching, coverslips were mounted in VECTASHIELD mounting medium (Vector Laboratories, Burlingame, CA). Pictures were taken with a fluorescence microscope equipped with a digital color camera (Nikon Eclipse 80i; Nikon Instruments Europe, Amstelveen, the Netherlands) using NIS Elements software (Nikon Instruments Europe). Cell surface area (CSA) and fluorescent intensity were measured using dedicated software (ImageJ, version 4.1 National Institutes of Health, Bethesda, MD). Data were obtained from four independent nr-vCMCs isolation.

Western blot analysis. Cardiomyocytes were lysed in 50 mmol/L Tris·HCl (pH 8.0), 150 mmol/L NaCl, 1% Triton X-100, 0.5% sodium deoxycholate, and 0.1% sodium dodecyl sulfate. Cell lysates were

Downloaded from journals.physiology.org/journal/jappl at Leids Univers Medisch Centrum (132.229.250.125) on January 11, 2023.

applied to a NuPAGE Novex 12% Bis-Tris gel (Life Technologies Europe). Following electrophoretic separation, the proteins were transferred to a polyvinylidene difluoride membrane (Amersham Hybond P; GE Healthcare Europe, Diegem, Belgium) by wet electroblotting. Next, membranes were blocked in Tris-based saline, 0.1% Tween-20, and 2% BSA (Sigma-Aldrich) for 1 h, at RT and probed with the same primary antibodies used for immunocytology (directed against NPPA, Serca2, and Acta1 (1:500, 1:2,000, and 1:500, respectively) and also mouse antiglyceraldehyde 3-phosphate dehydrogenase (GAPDH;1:10,000; Merck Millipore, Billerica, MA; clone 6C5), mouse anti-connexin 43 (Cx43; 1:120,000; Sigma-Aldrich), and rabbit anti cardiac voltage-gated sodium channel Nav1.5 (SCN5a; 1/500; Alomone Laboratory, Jerusalem, Israel; Asc-005) primary antibodies overnight at 4°C, followed by a 1-h incubation with appropriate horseradish peroxidase-conjugated secondary antibodies (Santa Cruz Biotechnology). Target protein signals were visualized using the Super Signal West Femto maximum sensitivity substrate kit (Thermo Scientific, Rockford, IL) and chemiluminescence was measured with the ChemiDoc XRS imaging system (Bio-Rad Laboratories, Veenendaal, the Netherlands). Cell isolation and treatment was repeated for three times. Three 15-mm wells, each seeded with 8×10^5 cells, were used for each sample.

Statistical analysis. Different experimental groups were compared using the unpaired samples *t*-test. Data were presented as means ± SD. Differences among means were considered significant at $P \leq 0.05$. Graphs were prepared in GraphPad Prism version 6 (GraphPad Software, La Jolla, CA).

RESULTS

PMA induces a hypertrophic response in nr-vCMCs. Immunostaining of control and PMA-treated nr-vCMC cultures for sarcomeric α-actinin showed the presence of ~13% nonmyocytes in the cultures (Fig. 1*A*). PMA treatment of nr-vCMC cultures did not show any cytotoxic effects (Fig. 1*B*), while it increased the mean cell surface area (CSA) by 30% [3.5 ± 1.5 ($n = 81$) vs. 2.6 ± 1.0 pixels in control cultures ($n = 54$), $P < 0.0005$] (Fig. 1*C*), and total protein content by 80% [1.3 ± 0.1 vs. 0.7 ± 0.1 mg/10^7 cells in control cultures ($n = 9$ for both experimental groups), $P < 0.0001$] (Fig. 1*D*), confirming that PMA is a hypertrophy inducer.

PMA-treated nr-vCMCs acquire a pathological hypertrophy-related phenotype. To investigate the nature of the hypertrophic response induced by PMA, control and drug-treated nr-vCMC cultures were immunostained for markers distinguishing physiological from pathological hypertrophy. The PMA-treated nr-vCMC cultures displayed a 42% increase in Nppa level [17.8 ± 2.0 vs. 12.5 ± 4.4 arbitrary units (AU), $P < 0.005$] (Fig. 2*A*), a 34% increase in Acta1 expression (22.0 ± 4.1 vs. 16.4 ± 2.6 AU, $P < 0.0005$) (Fig. 2*B*) and a 32% decrease in Serca2a level (15.9 ± 2.5 vs. 21.1 ± 3.5 AU, $P < 0.0001$) (Fig. 2*C*), as compared with those in control cultures. Assessment of the content of these proteins by Western blot analysis also showed increase in Nppa and Acta1 and decrease in Serca2a expression (Fig. 2*D*). This indicates that PMA-treated nr-vCMCs obtain properties of pathologically hypertrophic cardiac muscle cells.

Conduction and repolarization are slowed by PMA treatment of nr-vCMCs cultures. Optical mapping recordings in 1-Hz-paced, uniformly propagating nr-vCMC cultures showed that PMA treatment causes a strong reduction in CV (10 ± 4 vs. 21 ± 2 cm/s in control cultures, $P < 0.0001$) (Fig. 3*A*). Detection of the Cx43 and Nav1.5 proteins by Western blot analysis showed an increase in Cx43 level and decrease in Nav1.5 expression upon PMA treatment (Fig. 3*B*). Moreover,

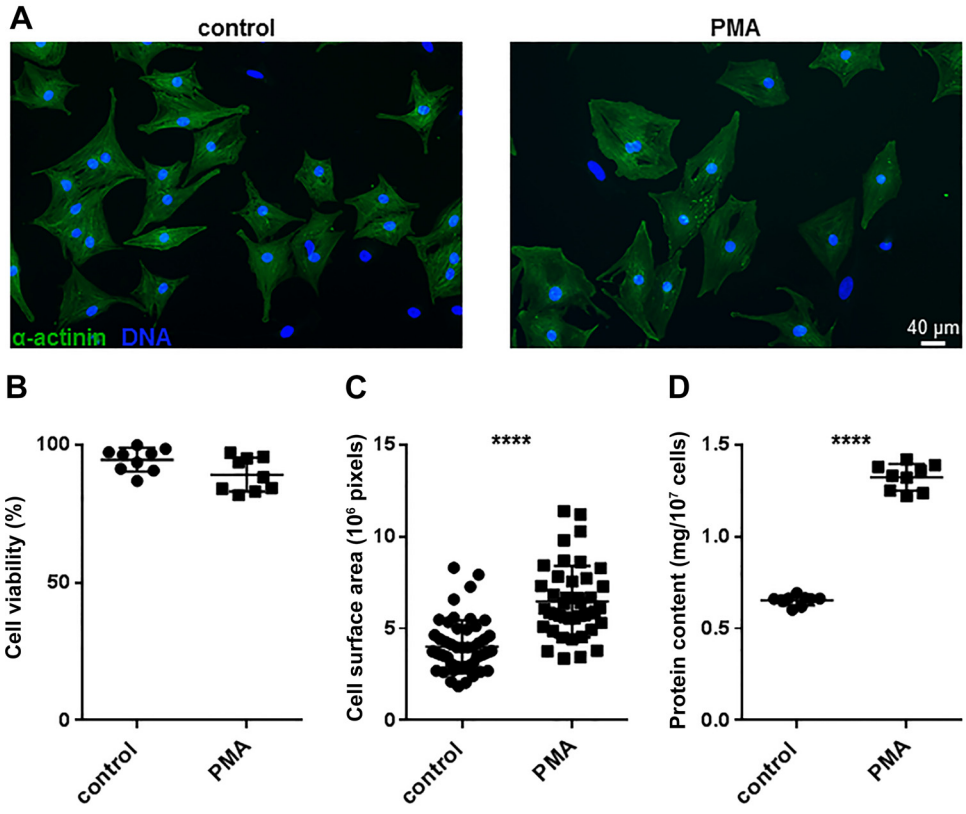

Fig. 1. Characterization of phorbol 12-myristate 13-acetate (PMA)-treated neonatal rat ventricular cardiomyocyte (nr-vCMC) cultures. *A*: α-actinin staining showed the presence of 13% nonmyocytes in the nr-vCMCs cultures. *B*: cell viability assay showed that PMA did not have any cytotoxic effects on nr-vCMC cultures. Quantification of cell surface area (CSA; *C*) and total protein content (*D*) of control and PMA-treated nr-vCMCs. CSA and protein level were increased in cultures treated with PMA, indicative of a hypertrophic response. ****$P < 0.0001$.

Downloaded from journals.physiology.org/journal/jappl at Leids Univers Medisch Centrum (132.229.250.125) on January 11, 2023.

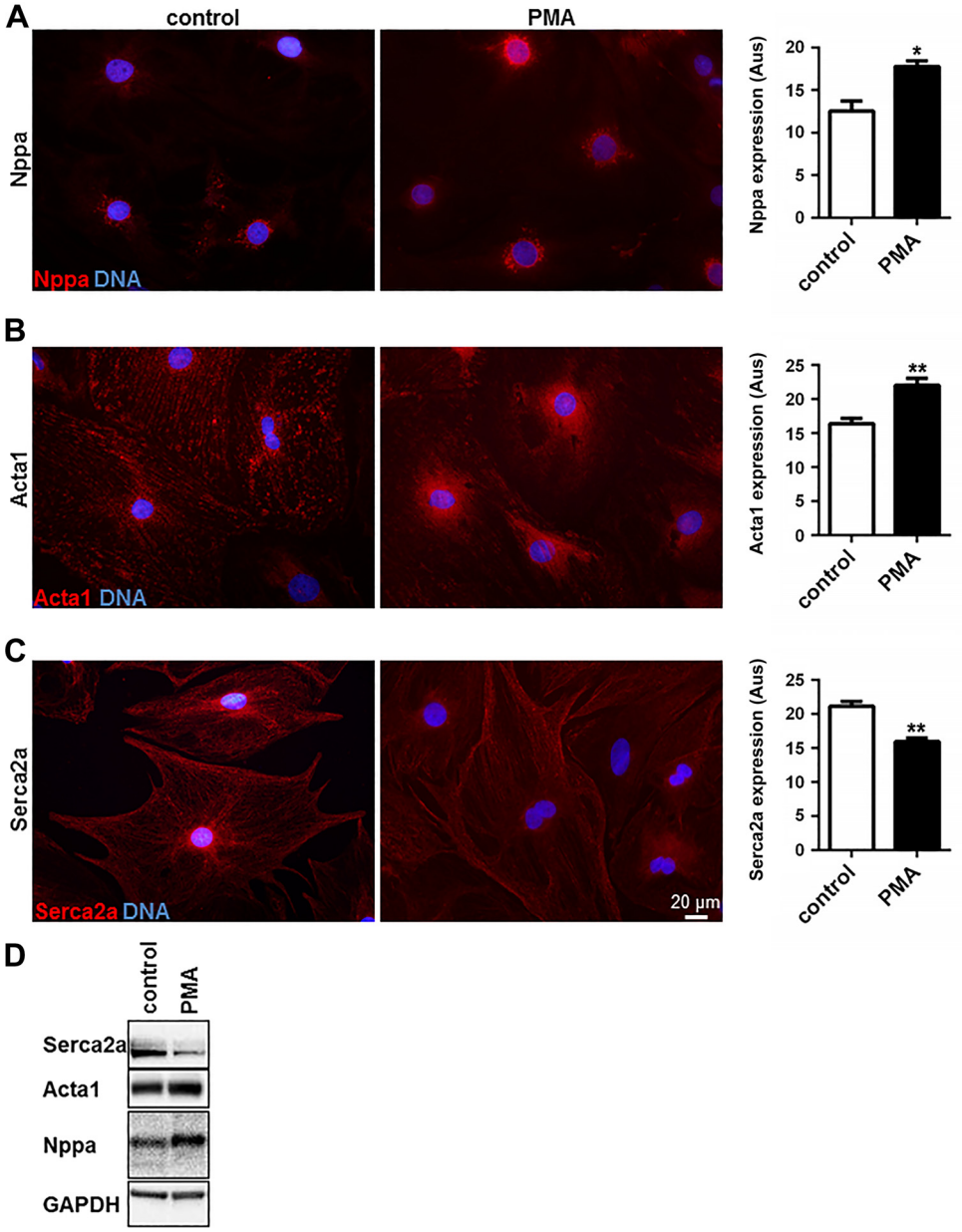

Fig. 2. Phorbol 12-myristate 13-acetate (PMA) treatment endows neonatal rat ventricular cardiomyocyte (nr-vCMCs) with features of pathological hypertrophied ventricular myocardium, including an increase in Nppa (42%) (*A*) and Acta1 (*B*) levels (34%) and a decrease in Serca2a (*C*) expression (32%). *D*: assessment of the content of Nppa, Acta1, and Serca2a proteins by Western blot analysis. $*P < 0.005$ and $**P < 0.0005$. AUs, arbitrary units.

the PMA-treated nr-vCMC cultures displayed a large increase in APD_{30} (306 ± 39 vs. 148 ± 18 ms in control cultures, $P < 0.0001$) and APD_{80} (516 ± 53 vs. 225 ± 34 ms in control cultures, $P < 0.0001$) (Fig. 3, *C* and *D* and Fig. 4*A*). Spatial APD dispersion was also increased in PMA-treated cultures (APD_{30} dispersion of 85 ± 19 vs. 22 ± 7 ms in control cultures, $P < 0.0001$ and APD_{80} dispersion of 50 ± 9 vs. 25 ± 2 ms in control cultures, $P < 0.0001$), implying increased heterogeneity of repolarization (Fig. 3, *C* and *D*).

Focal triggered activity is a prominent proarrhythmic feature of PMA-treated nr-vCMC cultures. The PMA-induced APD prolongation and increase in APD dispersion provided enough time and depolarizing force, respectively, for formation of early afterdepolarizations (EADs) in the drug-treated cultures, which could oscillate repetitively, resulting in focal tachyarrhythmias. The incidence of this type of arrhythmias following local 1-Hz stimulation was 53.6% in the PMA-treated nr-vCMC cultures ($n = 82$), while control nr-vCMC cultures showed 4.3% arrhythmias ($n = 70$) (Fig. 4, *A* and *B*). During focal tachyarrhythmias, repolarization halted at the initiation site of the EAD (Fig. 4*C*, *point 1*) followed by slow repolarization in areas in the vicinity of the region of sustained depolarization, which favored EAD formation (Fig. 4*C*, *point 2*).

DISCUSSION

The major findings of this study are *1*) exposure of nr-vCMC cultures for 2 times 24 h to PMA induces a hypertrophic response in the cardiac myocytes with hallmarks of pathological hypertrophied ventricular myocardium; *2*) following prolonged PMA treatment, nr-vCMC cultures undergo electrical remodeling, as evinced by a decrease in CV and an increase in APD and APD dispersion; *3*) PMA-treated nr-vCMC cultures

Downloaded from journals.physiology.org/journal/jappl at Leids Univers Medisch Centrum (132.229.250.125) on January 11, 2023.

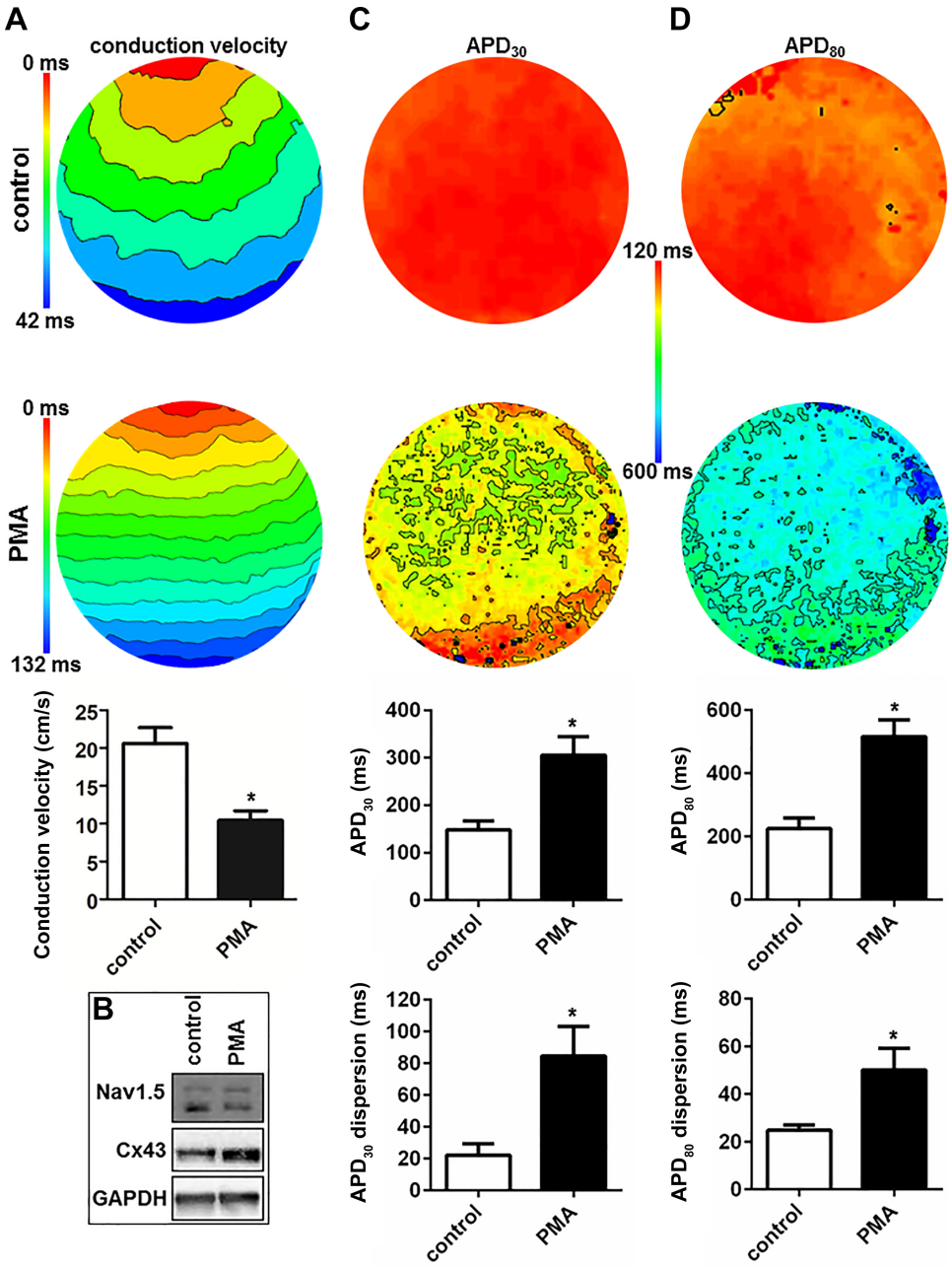

Fig. 3. Phorbol 12-myristate 13-acetate (PMA) treatment of neonatal rat ventricular cardiomyocyte (nr-vCMC) cultures causes conduction slowing and heterogeneous action potential duration (APD) prolongation. *A*: typical activation maps with 6-ms isochronal spacing and corresponding quantitative assessment of control and PMA-treated nr-vCMC cultures showing slowing of conduction upon PMA treatment. *B*: detection of the Cx43 and Nav1.5 proteins showing an increase in Cx43 level and decrease in Nav1.5 expression induced by PMA treatment. Typical APD_{30} (*C*) and APD_{80} (*D*) map of control and PMA-treated nr-vCMC cultures and corresponding quantitative assessments of APD and APD dispersion showing PMA-induced increases in APD and APD dispersion. Cultures were subjected to electrical point stimulation at a frequency of 1 Hz. $^*P < 0.0001$.

display a high incidence of triggered activity causing focal tachyarrhythmias; and *4*) mechanistically, the arrhythmias observed in nr-vCMC cultures rendered pathologically hypertrophic by prolonged PMA treatment are probably a direct consequence of the electrical remodeling process.

In vitro models of PCH. In recent years, much has been learned about the signaling pathways orchestrating both physiological and pathological heart growth (5). Through extensive molecular, genetic and pharmacological studies, G protein-coupled receptors (GPCRs) and their ligands [e.g., ANG II, ET-1, noradrenaline (NE)] have been identified as key regulators of PCH (39). This has led researchers to use these ligands or synthetic analogs hereof [e.g., isoproterenol, phenylephrine (PE)] to develop in vitro and in vivo models of PCH and heart failure (25, 30, 40, 54). In the in vitro models of pathological ventricular hypertrophy, an increase in CSA, mRNA and protein content, cell capacitance, and/or protein synthesis rate was taken as proof of cell growth, while increases in the expression of Nppa, natriuretic peptide precursor B (Nppb), Acta1, β-myosin heavy chain (Myh7), and/or decreases in α-myosin heavy chain (Myh6) and Serca2a levels were considered indicative of a pathological rather than a physiological hypertrophic response (29, 43).

The prohypertrophic effects of ANG II-, ET-1-, and catecholamine-binding GPCRs in the heart are in a large part attributable to the activation of phospholipase C, which converts phosphatidylinositol 4,5-bisphosphate (PIP_2) into the second messengers IP_3 and DAG. In this study, PCH was induced by using PMA as a synthetic analog of the second messenger DAG instead of by agonist-induced GPCR activation. Possible

Downloaded from journals.physiology.org/journal/jappl at Leids Univers Medisch Centrum (132.229.250.125) on January 11, 2023.

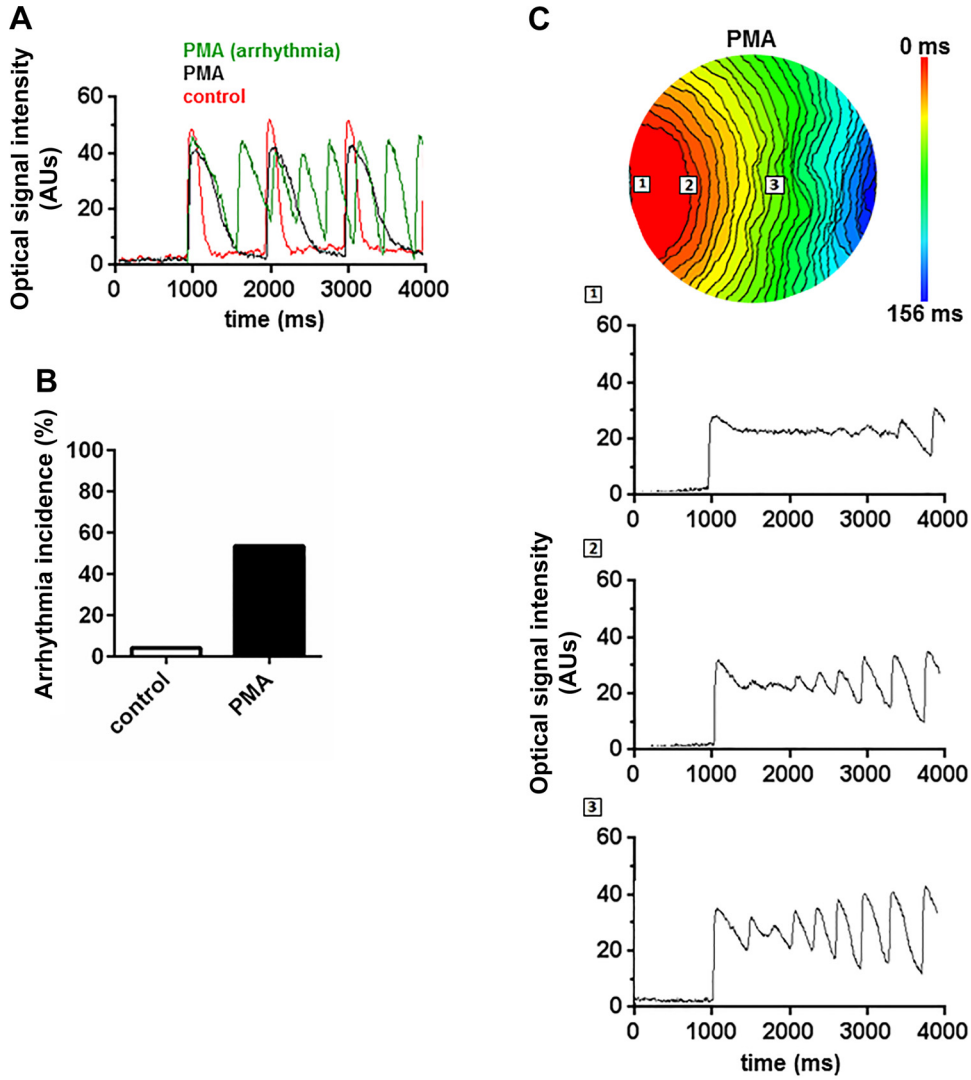

Fig. 4. Phorbol 12-myristate 13-acetate (PMA)-treated nr- neonatal rat ventricular cardiomyocyte (vCMC) cultures show a high incidence of focal tachyarrhythmias. *A*: typical optical signals are shown from control (red) and PMA-treated cultures showing APD prolongation (black) and onset of tachyarrhythmia (green). *B*: arrhythmia incidence (i.e., incidence of focal tachyarrhythmias) is quantified in control and PMA-treated nr-vCMC cultures. *C*: activation map shows a PMA-treated nr-vCMC culture displaying triggered activity. *Bottom*: corresponding optical signals show ceased repolarization (*point 1*), EAD initiation (*point 2*) and EAD propagation (*point 3*). AUs, arbitrary units.

prohypertrophic effects, caused by direct ligand-induced IP_3 receptor (IP_3R) activation and subsequent Ca^{2+} release, are, therefore, expected to be absent in our nr-vCMC-based PCH model. The PMA-treated nr-vCMC cultures, nevertheless, show a very robust hypertrophic response with hallmarks of PCH (Figs. 1 and 2), which is consistent with the results of previous studies that employed (prolonged) PMA treatment to render cardiomyocyte cultures hypertrophic (1, 20, 35–37). This suggests that either IP_3R signaling is not necessary for inducing PCH-related phenotypic changes in cultured nr-vCMCs or that IP_3Rs get activated by DAG-dependent signaling. Indeed, several studies have identified the DAG receptors PKC and PKD as important mediators of (pathological) cardiac hypertrophy, and fetal cardiac gene reactivation (15, 16, 31, 34, 44, 49). Consequently, overexpression of PKCα (7) or PKD3 (24) in nr-vCMCs induced pathological hypertrophic growth with increased fetal cardiac gene expression in these cells.

It has also been shown that GPCRs undergo nodal regulation following agonist activation induced by phosphorylation via family of kinases such as GPCR kinases (GRKs) (8, 38). GRK5 plays a key role in cardiac signaling regulation, and its expression is increased in heart failure. PMA, a known stimulator of NF-κB, increases the levels of GRK5 in myocytes, whereas treatment of cells with inhibitor of NF-κB or IκB kinase 2, decreases GRK5. Activity of NF-κB is increased in cardiac hypertrophy and enhanced GRK5, acting as a class II histone deacetylase (HDAC) kinase (27), can promote pathological ventricular hypertrophy and heart failure (22).

Proarrhythmic mechanisms of PCH. Despite the rapidly increasing knowledge about the molecular pathways involved in the development of PCH and heart failure, the mechanisms underlying electrical remodeling of the diseased heart are still poorly understood. This is partially due to the disparate results obtained in different in vivo studies focusing on PCH-related changes in cardiac electrophysiology (11, 26, 51). A confounding factor in these studies has been the use of different experimental conditions, animal models, and/or patient groups with distinct contributions of other factors besides PCH to the electrophysiological remodeling process. In this study, using a well-defined in vitro model system, heterogeneous APD prolongation, and EAD-triggered activity were identified as likely key players in the development of PCH-associated arrhythmias. These findings are consistent with the results of animal and clinical studies attributing a prominent role of EADs to the

Downloaded from journals.physiology.org/journal/jappl at Leids Univers Medisch Centrum (132.229.250.125) on January 11, 2023.

development of ventricular tachyarrhythmias (3, 10, 53). In our study, given the pronounced elongation of phase 2 of the AP in the PMA-treated nr-vCMCs, L-type Ca^{2+} channels and delayed rectifier K^+ channels (53) are probably the ionic basis of the EADs. In support of this idea, Puglisi et al. (36) recently showed that chronic exposure (i.e., for 48–72 h) of nr-vCMCs to PMA caused a strong decrease in normalized I_{Ks}. The same researchers also reported a significant decrease in I_{to} and a substantial increase in $I_{Na^+/Ca^{2+}}$, while the normalized $I_{Ca,L}$ did not change significantly. A decrease in I_{to} following overnight exposure of nr-vCMCs to PMA has also been documented by Walsh et al. (50). Reduction in Serca2a expression is proportional to the extent of pathological hypertrophy. Another important result observed in our PMA-treated nr-vCMCs was a 32% decrease in Serca2a protein level. Similar findings were made by Porter et al. (34) and Qi et al. (37) following prolonged treatment of nr-vCMCs with PMA. In their study, Qi et al. found that the reduction in Serca2a expression led to a slowing of diastolic Ca^{2+} uptake into the sarcoplasmic reticulum with possible proarrhythmic consequences. Besides the reduced repolarization reserve at the earlier phases of repolarization (i.e., between −40 and 0 mV) and the increased APD dispersion, also the conduction slowing is a major risk factor for the development of ventricular tachyarrhythmias (48). Interstitial fibrosis and collagen deposition occurring in severe LVH, disturb the conduction by a decrease in gap junctional proteins and change in their distribution, therefore, providing conditions for reentry circuits (48, 52). In our study, detection of the Cx43 protein level showed an increase upon PMA treatment; therefore, the most likely explanation for the conduction slowing observed in our PMA-treated nr-vCMC cultures is downregulation of Nav1.5 protein level, as has been observed in cardiac conduction defects and ventricular tachycardia (32, 41, 46). Therefore, decrease in the amplitude of the upstroke phase of the action potential upon PMA treatment (Fig. 4*A*) could be the result of decrease in Nav1.5 protein expression.

PCH versus heart failure model. In response to hemodynamic stress and/or myocardial injury (i.e., when cardiac load exceeds cardiac output) the heart engages in a process called compensatory hypertrophy through the enlargement of cardiomyocytes by the parallel (concentric hypertrophy) or serial (eccentric hypertrophy) addition of sarcomeres. This process is under neurohormonal control of the adrenergic nervous system and renin-angiotensin system. At the molecular level, the changes in cardiomyocyte phenotype are accompanied by reinduction of the so-called fetal gene program, because patterns of gene expression mimic those observed during cardiac development. In the continued presence of pathological stimuli, excessive cardiomyocyte death will provoke transition to dilated cardiomyopathy, leading to heart failure. The latter process is associated with functional perturbations of cellular Ca^{2+} homeostasis and ionic currents, resulting in impaired force generation and the development of malignant arrhythmias (12, 51). The PMA-treated nr-vCMC cultures display many of the same electrophysiological changes found in moderate PCH, including heterogeneous APD prolongation and a high incidence of EAD-triggered activity. This may suggest that the PMA-treated nr-vCMC cultures represent a relatively middle stage in the transition from PCH to heart failure. Further evidence for this presupposition should come from a comparison of the contractile force-generating capacity of control and PMA-treated nr-vCMC cultures and from comparative transcriptome analyses.

Conclusion. In the present study, treatment of nr-vCMCs twice in 24 h with PMA not only promoted cardiomyocyte hypertrophy but also led to the reactivation of fetal cardiac genes, as evinced by PMA-dependent increases in Nppa and Acta1 levels and a decrease in Serca2a expression. PMA-treated nr-vCMCs showed a high incidence of triggered tachyarrhythmias associated with increases in APD and APD dispersion, caused by electrical remodeling. To the best of our knowledge, this is the first study in which the proarrhythmic features of PCH per se have been investigated. Since this in vitro model of PCH is highly controllable and provides reproducible results, it is ideally suited for testing in proof-of-concept studies new therapeutic interventions (genetic modifications or pharmacological treatments) that target specific aspects of moderate hypertrophy-associated arrhythmias independent of fibrosis, collagen deposition, or other PCH-related processes, which occur in severe left ventricular hypertrophy.

Study limitations. In this study, PCH-related arrhythmias were investigated in two-dimensional cultures of nr-vCMCs. Although this in vitro model system has greatly contributed to our current understanding of heart structure and function and lends itself very well to pharmacological and genetic manipulation, the electrophysiological properties of PMA-treated nr-vCMCs will only partially resemble those of cardiomyocytes in the pathologically hypertrophied human heart. Also, in isolation, pathological hypertrophy may have a different impact on cardiomyocytes' behavior than in combination with other cardiac pathologies like inflammation, hypoxia, and fibrosis. Accordingly, discoveries made in PMA-treated nr-vCMC cultures will always have to be verified in more clinically relevant settings. Even so, because of the relative ease with which nr-vCMCs can be obtained, cultured, and manipulated, they represent a highly useful model system for mechanistic and therapy-directed cardiac research.

GRANTS

This work was supported by an unrestricted research grant from the Iranian Ministry of Science, Research and Technology.

DISCLOSURES

No conflicts of interest, financial or otherwise, are declared by the authors.

AUTHOR CONTRIBUTIONS

Z.N. and A.A.F.d.V. conceived and designed research; Z.N. performed experiments; Z.N. analyzed data; Z.N. and A.A.F.d.V. interpreted results of experiments; Z.N. prepared figures; Z.N. drafted manuscript; M.J.S. and A.A.F.d.V. edited and revised manuscript; Z.N., M.J.S., and A.A.F.d.V. approved final version of manuscript.

REFERENCES

1. **Allo SN, Carl LL, Morgan HE.** Acceleration of growth of cultured cardiomyocytes and translocation of protein kinase C. *Am J Physiol Cell Physiol* 263: C319–C325, 1992. doi:10.1152/ajpcell.1992.263.2.C319.
2. **Amano Y, Kitamura M, Tachi M, Takeda M, Mizuno K, Kumita S.** Delayed enhancement magnetic resonance imaging in hypertrophic cardiomyopathy with basal septal hypertrophy and preserved ejection fraction: relationship with ventricular tachyarrhythmia. *J Comput Assist Tomogr* 38: 67–71, 2014. doi:10.1097/RCT.0b013e3182a2fb01.

Downloaded from journals.physiology.org/journal/jappl at Leids Univers Medisch Centrum (132.229.250.125) on January 11, 2023.

3. **Antoons G, Volders PG, Stankovicova T, Bito V, Stengl M, Vos MA, Sipido KR.** Window Ca^{2+} current and its modulation by Ca^{2+} release in hypertrophied cardiac myocytes from dogs with chronic atrioventricular block. *J Physiol* 579: 147–160, 2007. doi:10.1113/jphysiol.2006.124222.
4. **Arnol M, Starc V, Knap B, Potocnik N, Bren AF, Kandus A.** Left ventricular mass is associated with ventricular repolarization heterogeneity one year after renal transplantation. *Am J Transplant* 8: 446–451, 2008. doi:10.1111/j.1600-6143.2007.02083.x.
5. **Bernardo BC, Weeks KL, Pretorius L, McMullen JR.** Molecular distinction between physiological and pathological cardiac hypertrophy: experimental findings and therapeutic strategies. *Pharmacol Ther* 128: 191–227, 2010. doi:10.1016/j.pharmthera.2010.04.005.
6. **Blum JL, Samarel AM, Mestril R.** Phosphorylation and binding of AUF1 to the 3′-untranslated region of cardiomyocyte SERCA2a mRNA. *Am J Physiol Heart Circ Physiol* 289: H2543–H2550, 2005. doi:10.1152/ajpheart.00545.2005.
7. **Braz JC, Bueno OF, De Windt LJ, Molkentin JD.** PKC α regulates the hypertrophic growth of cardiomyocytes through extracellular signal-regulated kinase1/2 (ERK1/2). *J Cell Biol* 156: 905–919, 2002. doi:10.1083/jcb.200108062.
8. **Brinks H, Koch WJ.** Targeting G protein-coupled receptor kinases (GRKs) in heart failure. *Drug Discov Today Dis Mech* 7: e129–e134, 2010. doi:10.1016/j.ddmec.2010.07.007.
9. **Burchfield JS, Xie M, Hill JA.** Pathological ventricular remodeling: mechanisms: part 1 of 2. *Circulation* 128: 388–400, 2013. doi:10.1161/CIRCULATIONAHA.113.001878.
10. **Cosín Aguilar J, Hernandiz Martinez A, Andres Conejos F.** Mechanisms of ventricular arrhythmias in the presence of pathological hypertrophy. *Eur Heart J* 14, *Suppl J*: 65–70, 1993.
11. **Cutler MJ, Jeyaraj D, Rosenbaum DS.** Cardiac electrical remodeling in health and disease. *Trends Pharmacol Sci* 32: 174–180, 2011. doi:10.1016/j.tips.2010.12.001.
12. **Diwan A, Dorn GW II.** Decompensation of cardiac hypertrophy: cellular mechanisms and novel therapeutic targets. *Physiology (Bethesda)* 22: 56–64, 2007. doi:10.1152/physiol.00033.2006.
13. **Doble BW, Ping P, Fandrich RR, Cattini PA, Kardami E.** Protein kinase C-epsilon mediates phorbol ester-induced phosphorylation of connexin-43. *Cell Commun Adhes* 8: 253–256, 2001. doi:10.3109/15419060109080733.
14. **Dunnmon PM, Iwaki K, Henderson SA, Sen A, Chien KR.** Phorbol esters induce immediate-early genes and activate cardiac gene transcription in neonatal rat myocardial cells. *J Mol Cell Cardiol* 22: 901–910, 1990. doi:10.1016/0022-2828(90)90121-H.
15. **Ellwanger K, Hausser A.** Physiological functions of protein kinase D in vivo. *IUBMB Life* 65: 98–107, 2013. doi:10.1002/iub.1116.
16. **Fielitz J, Kim MS, Shelton JM, Qi X, Hill JA, Richardson JA, Bassel-Duby R, Olson EN.** Requirement of protein kinase D1 for pathological cardiac remodeling. *Proc Natl Acad Sci USA* 105: 3059–3063, 2008. doi:10.1073/pnas.0712265105.
17. **Galinier M, Balanescu S, Fourcade J, Dorobantu M, Albenque JP, Massabuau P, Doazan JP, Fauvel JM, Bounhoure JP.** Prognostic value of arrhythmogenic markers in systemic hypertension. *Eur Heart J* 18: 1484–1491, 1997. doi:10.1093/oxfordjournals.eurheartj.a015476.
18. **Grossman W, Jones D, McLaurin LP.** Wall stress and patterns of hypertrophy in the human left ventricle. *J Clin Invest* 56: 56–64, 1975. doi:10.1172/JCI108079.
19. **Haider AW, Larson MG, Benjamin EJ, Levy D.** Increased left ventricular mass and hypertrophy are associated with increased risk for sudden death. *J Am Coll Cardiol* 32: 1454–1459, 1998. doi:10.1016/S0735-1097(98)00407-0.
20. **Hartong R, Villarreal FJ, Giordano F, Hilal-Dandan R, McDonough PM, Dillmann WH.** Phorbol myristate acetate-induced hypertrophy of neonatal rat cardiac myocytes is associated with decreased sarcoplasmic reticulum Ca^{2+} ATPase (SERCA2) gene expression and calcium reuptake. *J Mol Cell Cardiol* 28: 2467–2477, 1996. doi:10.1006/jmcc.1996.0239.
21. **Hohendanner F, McCulloch AD, Blatter LA, Michailova AP.** Calcium and IP3 dynamics in cardiac myocytes: experimental and computational perspectives and approaches. *Front Pharmacol* 5: 35, 2014. doi:10.3389/fphar.2014.00035.
22. **Islam KN, Koch WJ.** Involvement of nuclear factor-κB (NF-κB) signaling pathway in regulation of cardiac G protein-coupled receptor kinase 5 (GRK5) expression. *J Biol Chem* 287: 12771–12778, 2012. doi:10.1074/jbc.M111.324566.
23. **Kwak BR, van Veen TA, Analbers LJ, Jongsma HJ.** TPA increases conductance but decreases permeability in neonatal rat cardiomyocyte gap junction channels. *Exp Cell Res* 220: 456–463, 1995. doi:10.1006/excr.1995.1337.
24. **Li C, Li J, Cai X, Sun H, Jiao J, Bai T, Zhou XW, Chen X, Gill DL, Tang XD.** Protein kinase D3 is a pivotal activator of pathological cardiac hypertrophy by selectively increasing the expression of hypertrophic transcription factors. *J Biol Chem* 286: 40782–40791, 2011. doi:10.1074/jbc.M111.263046.
25. **Lijnen P, Petrov V.** Renin-angiotensin system, hypertrophy and gene expression in cardiac myocytes. *J Mol Cell Cardiol* 31: 949–970, 1999. doi:10.1006/jmcc.1999.0934.
26. **Liu HB, Yang BF, Dong DL.** Calcineurin and electrical remodeling in pathologic cardiac hypertrophy. *Trends Cardiovasc Med* 20: 148–153, 2010. doi:10.1016/j.tcm.2010.12.003.
27. **Martini JS, Raake P, Vinge LE, DeGeorge BR Jr, Chuprun JK, Harris DM, Gao E, Eckhart AD, Pitcher JA, Koch WJ.** Uncovering G protein-coupled receptor kinase-5 as a histone deacetylase kinase in the nucleus of cardiomyocytes. *Proc Natl Acad Sci USA* 105: 12457–12462, 2008. doi:10.1073/pnas.0803153105.
28. **McLenachan JM, Dargie HJ.** Determinants of ventricular arrhythmias in cardiac hypertrophy. *J Cardiovasc Pharmacol* 17, *Suppl* 2: S46–S49, 1991. doi:10.1097/00005344-199117002-00011.
29. **Mendes P, Martinho R, Leite S, Maia-Moço L, Leite-Moreira AF, Lourenço AP, Moreira-Rodrigues M.** Chronic exercise induces pathological left ventricular hypertrophy in adrenaline-deficient mice. *Int J Cardiol* 253: 113–119, 2018. doi:10.1016/j.ijcard.2017.10.014.
30. **Osadchii OE.** Cardiac hypertrophy induced by sustained β-adrenoreceptor activation: pathophysiological aspects. *Heart Fail Rev* 12: 66–86, 2007. doi:10.1007/s10741-007-9007-4.
31. **Palaniyandi SS, Sun L, Ferreira JC, Mochly-Rosen D.** Protein kinase C in heart failure: a therapeutic target? *Cardiovasc Res* 82: 229–239, 2009. doi:10.1093/cvr/cvp001.
32. **Papadatos GA, Wallerstein PM, Head CE, Ratcliff R, Brady PA, Benndorf K, Saumarez RC, Trezise AE, Huang CL, Vandenberg JI, Colledge WH, Grace AA.** Slowed conduction and ventricular tachycardia after targeted disruption of the cardiac sodium channel gene Scn5a. *Proc Natl Acad Sci USA* 99: 6210–6215, 2002. doi:10.1073/pnas.082121299.
33. **Pijnappels DA, Schalij MJ, Ramkisoensing AA, van Tuyn J, de Vries AA, van der Laarse A, Ypey DL, Atsma DE.** Forced alignment of mesenchymal stem cells undergoing cardiomyogenic differentiation affects functional integration with cardiomyocyte cultures. *Circ Res* 103: 167–176, 2008. doi:10.1161/CIRCRESAHA.108.176131.
34. **Porter MJ, Heidkamp MC, Scully BT, Patel N, Martin JL, Samarel AM.** Isoenzyme-selective regulation of SERCA2 gene expression by protein kinase C in neonatal rat ventricular myocytes. *Am J Physiol Cell Physiol* 285: C39–C47, 2003. doi:10.1152/ajpcell.00461.2002.
35. **Prasad AM, Inesi G.** Regulation and rate limiting mechanisms of Ca^{2+} ATPase (SERCA2) expression in cardiac myocytes. *Mol Cell Biochem* 361: 85–96, 2012. doi:10.1007/s11010-011-1092-y.
36. **Puglisi JL, Yuan W, Timofeyev V, Myers RE, Chiamvimonvat N, Samarel AM, Bers DM.** Phorbol ester and endothelin-1 alter functional expression of Na^+/Ca^{2+} exchange, K^+, and Ca^{2+} currents in cultured neonatal rat myocytes. *Am J Physiol Heart Circ Physiol* 300: H617–H626, 2011. doi:10.1152/ajpheart.00388.2010.
37. **Qi M, Bassani JW, Bers DM, Samarel AM.** Phorbol 12-myristate 13-acetate alters SR Ca^{2+}-ATPase gene expression in cultured neonatal rat heart cells. *Am J Physiol* 271: H1031–H1039, 1996. doi:10.1152/ajpheart.1996.271.3.H1031.
38. **Rockman HA, Koch WJ, Lefkowitz RJ.** Seven-transmembrane-spanning receptors and heart function. *Nature* 415: 206–212, 2002. doi:10.1038/415206a.
39. **Salazar NC, Chen J, Rockman HA.** Cardiac GPCRs: GPCR signaling in healthy and failing hearts. *Biochim Biophys Acta* 1768: 1006–1018, 2007. doi:10.1016/j.bbamem.2007.02.010.
40. **Schaub MC, Hefti MA, Harder BA, Eppenberger HM.** Various hypertrophic stimuli induce distinct phenotypes in cardiomyocytes. *J Mol Med (Berl)* 75: 901–920, 1997. doi:10.1007/s001090050182.
41. **Schott JJ, Alshinawi C, Kyndt F, Probst V, Hoorntje TM, Hulsbeek M, Wilde AA, Escande D, Mannens MM, Le Marec H.** Cardiac conduction defects associate with mutations in SCN5A. *Nat Genet* 23: 20–21, 1999. doi:10.1038/12618.

Downloaded from journals.physiology.org/journal/jappl at Leids Univers Medisch Centrum (132.229.250.125) on January 11, 2023.

42. **Shigekawa M, Katanosaka Y, Wakabayashi S.** Regulation of the cardiac Na^+/Ca^{2+} exchanger by calcineurin and protein kinase C. *Ann N Y Acad Sci* 1099: 53–63, 2007. doi:10.1196/annals.1387.059.
43. **Shimizu I, Minamino T.** Physiological and pathological cardiac hypertrophy. *J Mol Cell Cardiol* 97: 245–262, 2016. doi:10.1016/j.yjmcc.2016.06.001.
44. **Shubeita HE, Martinson EA, Van Bilsen M, Chien KR, Brown JH.** Transcriptional activation of the cardiac myosin light chain 2 and atrial natriuretic factor genes by protein kinase C in neonatal rat ventricular myocytes. *Proc Natl Acad Sci USA* 89: 1305–1309, 1992. doi:10.1073/pnas.89.4.1305.
45. **Sin YY, Baillie GS.** Protein kinase D in the hypertrophy pathway. *Biochem Soc Trans* 40: 287–289, 2012. doi:10.1042/BST20110626.
46. **Song W, Shou W.** Cardiac sodium channel Nav1.5 mutations and cardiac arrhythmia. *Pediatr Cardiol* 33: 943–949, 2012. doi:10.1007/s00246-012-0303-y.
47. **Steinberg SF.** Cardiac actions of protein kinase C isoforms. *Physiology (Bethesda)* 27: 130–139, 2012. doi:10.1152/physiol.00009.2012.
48. **van Rijen HV, Eckardt D, Degen J, Theis M, Ott T, Willecke K, Jongsma HJ, Opthof T, de Bakker JM.** Slow conduction and enhanced anisotropy increase the propensity for ventricular tachyarrhythmias in adult mice with induced deletion of connexin43. *Circulation* 109: 1048–1055, 2004. doi:10.1161/01.CIR.0000117402.70689.75.
49. **Vega RB, Harrison BC, Meadows E, Roberts CR, Papst PJ, Olson EN, McKinsey TA.** Protein kinases C and D mediate agonist-dependent cardiac hypertrophy through nuclear export of histone deacetylase 5. *Mol Cell Biol* 24: 8374–8385, 2004. doi:10.1128/MCB.24.19.8374-8385.2004.
50. **Walsh KB, Sweet JK, Parks GE, Long KJ.** Modulation of outward potassium currents in aligned cultures of neonatal rat ventricular myocytes during phorbol ester-induced hypertrophy. *J Mol Cell Cardiol* 33: 1233–1247, 2001. doi:10.1006/jmcc.2001.1386.
51. **Wang Y, Hill JA.** Electrophysiological remodeling in heart failure. *J Mol Cell Cardiol* 48: 619–632, 2010. doi:10.1016/j.yjmcc.2010.01.009.
52. **Weber KT, Brilla CG.** Pathological hypertrophy and cardiac interstitium. Fibrosis and renin-angiotensin-aldosterone system. *Circulation* 83: 1849–1865, 1991. doi:10.1161/01.CIR.83.6.1849.
53. **Weiss JN, Garfinkel A, Karagueuzian HS, Chen PS, Qu Z.** Early afterdepolarizations and cardiac arrhythmias. *Heart Rhythm* 7: 1891–1899, 2010. doi:10.1016/j.hrthm.2010.09.017.
54. **Wollert KC, Drexler H.** The renin-angiotensin system and experimental heart failure. *Cardiovasc Res* 43: 838–849, 1999. doi:10.1016/S0008-6363(99)00145-5.

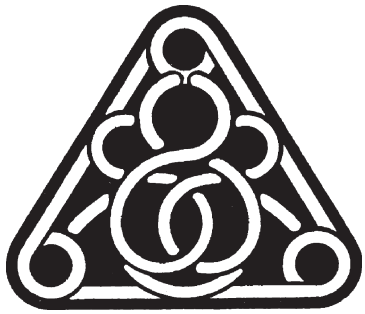

Downloaded from journals.physiology.org/journal/jappl at Leids Univers Medisch Centrum (132.229.250.125) on January 11, 2023.